US-Japan Exchange Workshop on New directions and physics for compact toroids

September 14-16, 2004, at LaFonda Hotel, Santa Fe, NM

Asymmetrical Structures inside the Separatrix on Field-Reversed Configuration Plasmas

Hiroshi Gota, Tomohiko Asai, Tsutomu Takahashi, and Yasuyuki Nogi

College of Science and Technology, Nihon University, Tokyo 101-8308, Japan

Outline

- Background and purpose
- Experimental apparatus and typical plasma parameters
- Separatrix shapes and internal structures
- Optical diagnostics
- Asymmetrical profiles and nonconcentric structures
- Summary

CST www.cst.nihon-u.ac.jp

日本大学 理工学部 NIHON UNIVERSITY COLLEGE OF SCIENCE AND TECHNOLOGY

Background and Purpose

- Separatrix shape of a field-reversed configuration (FRC) plasma is determined approximately by using an excluded flux measurement; then, we developed a new measurement, which called iterative method, to determine the separatrix shape and the internal structure of FRC with high accuracy. This method compares the measured magnetic fluxes with the solution of the Grad-Shafranov equation. From the analysis, it is found that there are the **magnetic islands** near the field null not only at the formation phase but also at the quiescent phase.

- To study precisely the **internal structures**, we measure the radiation of FRC plasma by using an optical diagnostic system and compare with the magnetic structure inside the separatrix. We also discuss the global motions inside the separatrix in order to confirm the asymmetrical radiation profiles at end regions of FRC plasma.

Experimental Apparatus

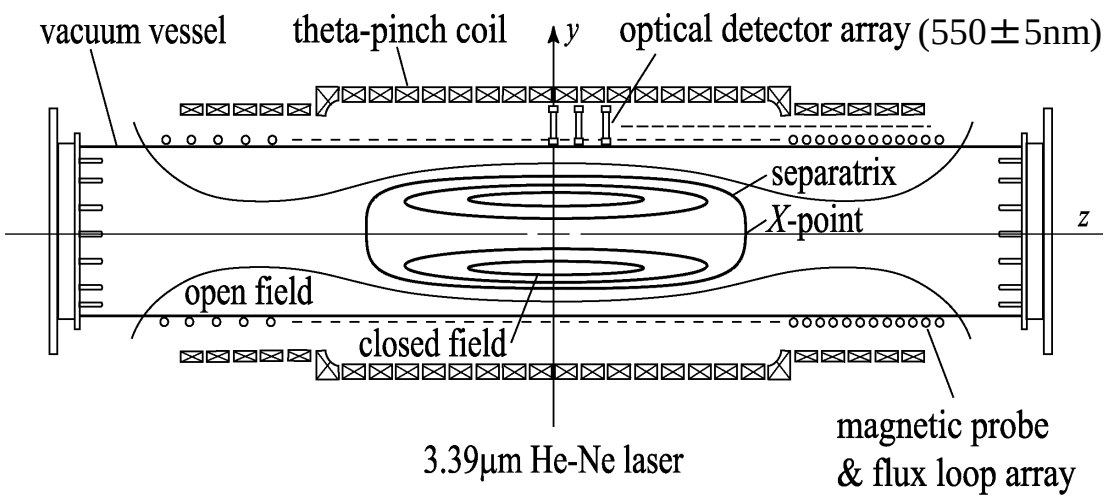

Fig. 1. FRC plasma on NUCTE-III.

Device parameters

Coil radius	:	0.17m, 0.15m
Coil length	:	1.54m
z-discharge	:	44kA
Bias field	:	-0.032T
Main field	:	0.6T (at peak)

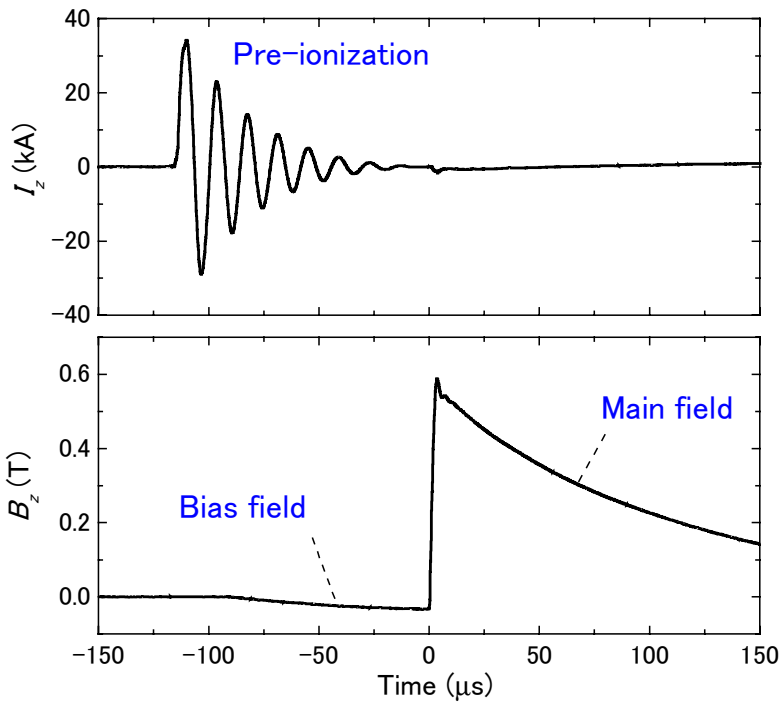

Fig. 2. Time sequence of discharge.

Plasma Parameters

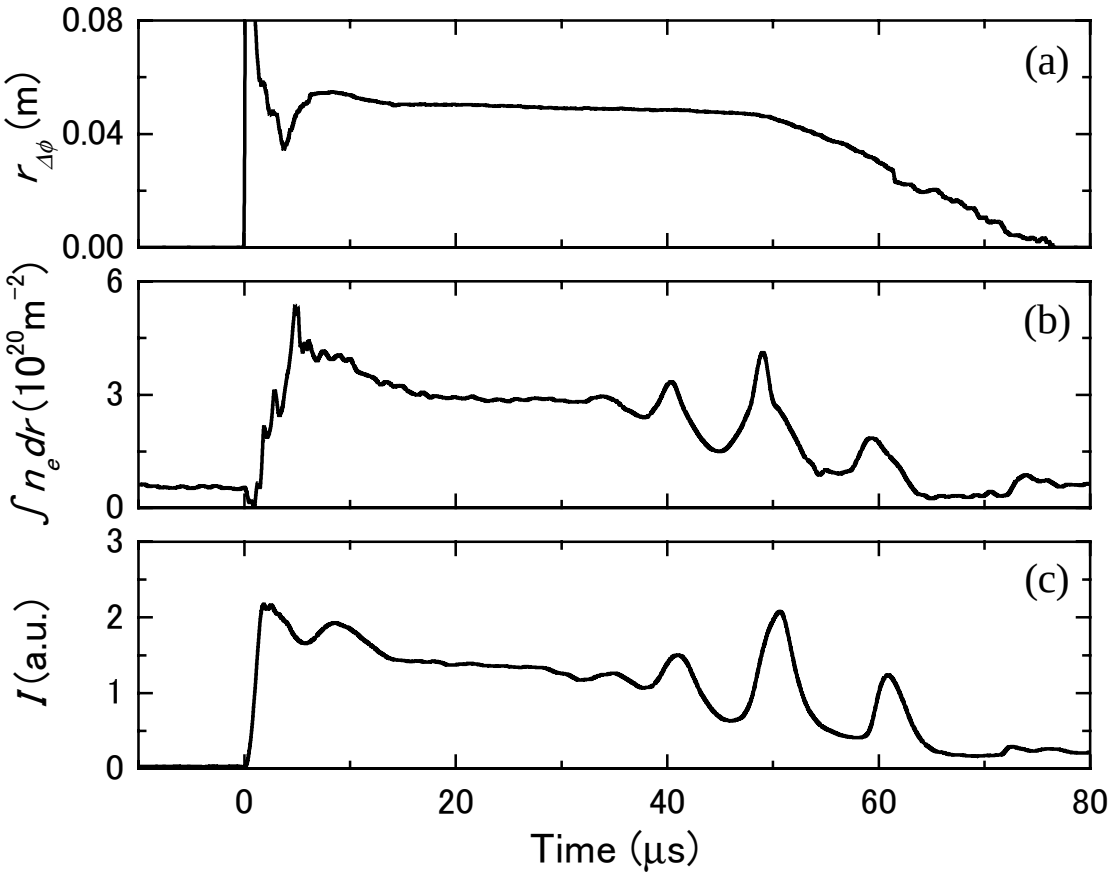

Excluded flux radius

$$r_{\Delta\Phi} = r_l \sqrt{1 - \frac{\Phi_p B_{zv}}{\Phi_v B_{zp}}}$$

Plasma parameters

Radius : ~0.05m ($x_s \approx 0.3$)
Length : ~0.8m
Electron density : ~3×10^{21}m^{-3}
Configuration life time : ~70μs
Electron and Ion temperatures : ~200eV

Fig. 3. Typical plasma parameters on NUCTE-III; (a) excluded flux radius, (b) line-integrated electron density and (c) line-integrated radiation intensity.

Estimation of Magnetic Structure

Grad-Shafranov equation

$$\frac{\partial^2\psi}{\partial r^2}-\frac{1}{r}\frac{\partial\psi}{\partial r}+\frac{\partial^2\psi}{\partial z^2}+\mu_0 r^2\frac{\partial p(\psi)}{\partial\psi}=0$$

< Pressure profiles >

$$p(\psi)=\begin{cases} p_s\exp\{(-\log\beta_s/\psi_n)\psi\} & \psi<0 \\ p_s\exp\{-2\psi/\psi_{edge}\} & 0\le\psi\le\psi_{edge} \\ 0 & \psi_{edge}<\psi \end{cases}$$

Where,

$$r(\psi_{edge})=r_s+w\rho_i$$

$$\psi_n\approx -0.01$$

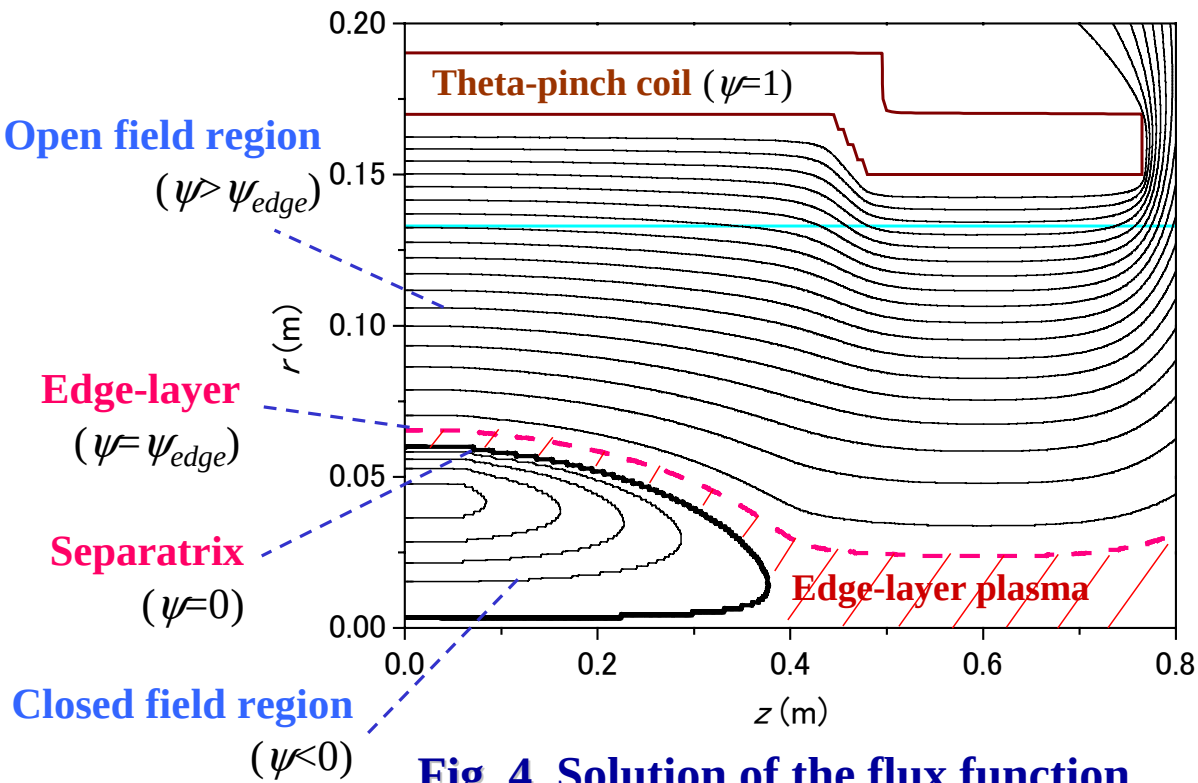

Fig. 4. Solution of the flux function.

When we use B_e=0.5 T and ρ_i=4.1 mm, it is obtained that the parameters of **β_s=0.7** and **w=4** are optimum values.

- ✓ H. Gota *et al.*, Rev. Sci. Instrum. **74**, 2318 (2003)
- ✓ H. Gota *et al.*, Phys Plasmas **10**, 4763 (2003)

Magnetic Structure inside the Separatrix

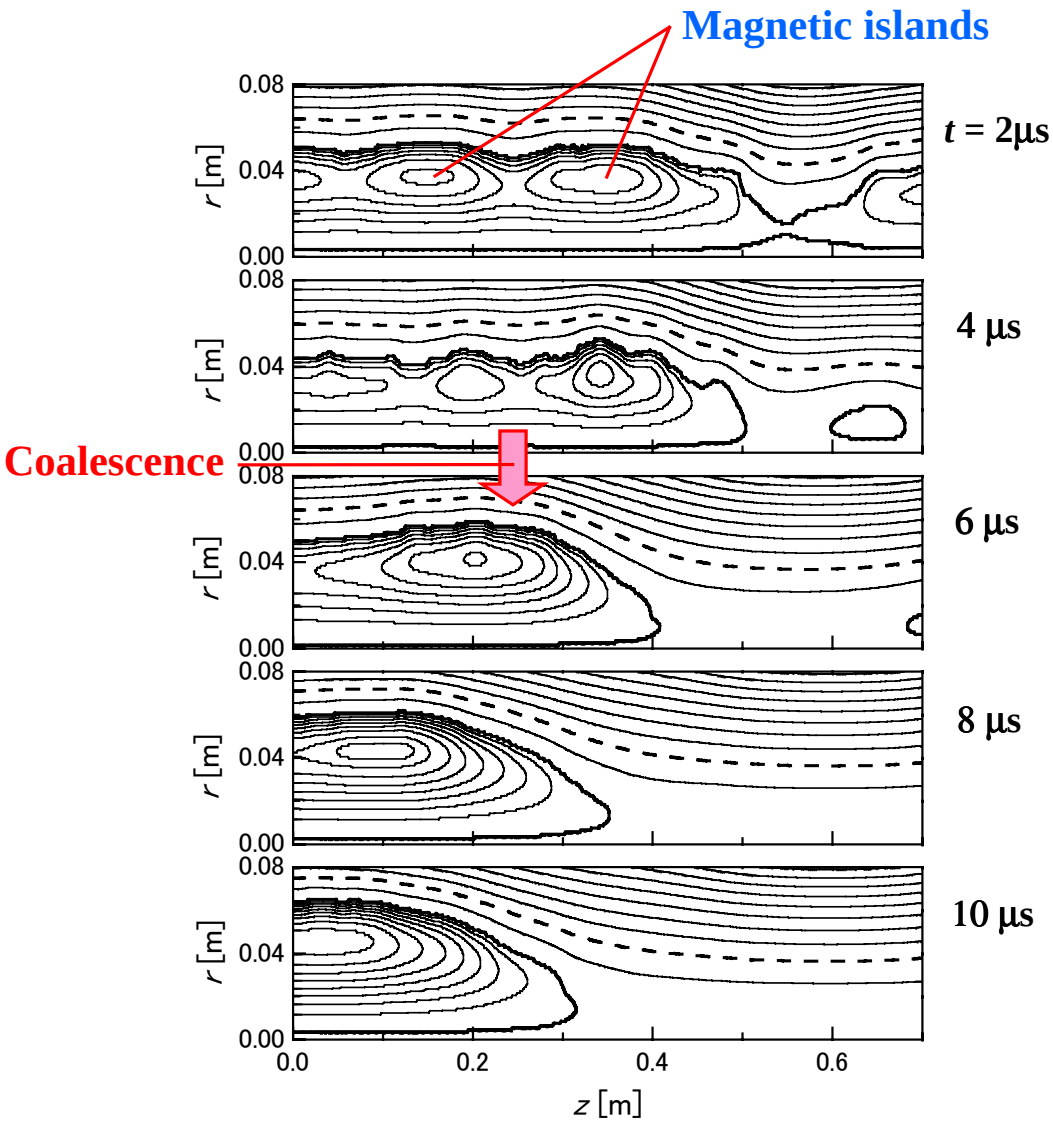

Fig. 5. Magnetic structures at the formation phase.

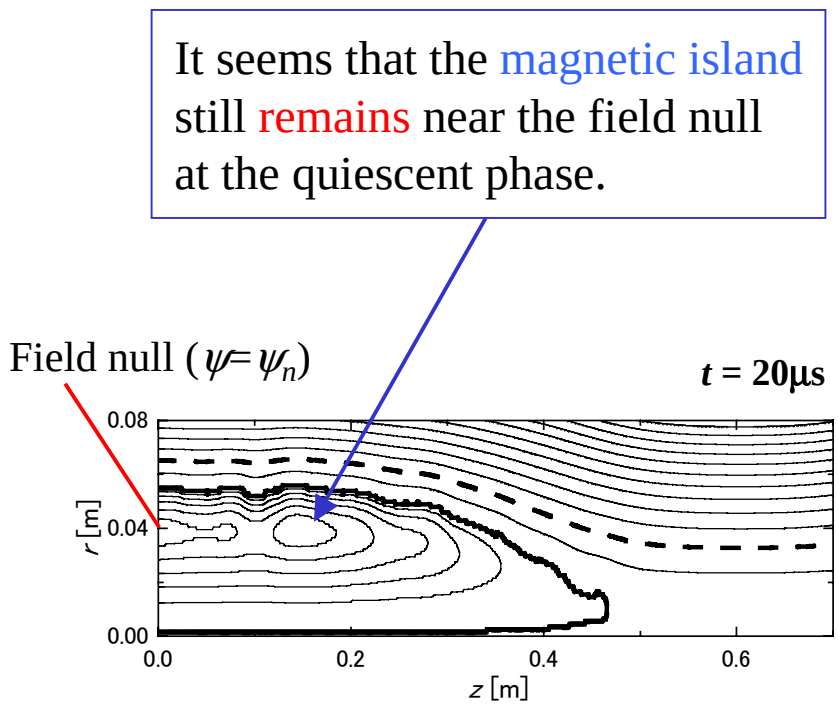

Fig. 6. Magnetic structures at the quiescent phase.

Optical Diagnostics

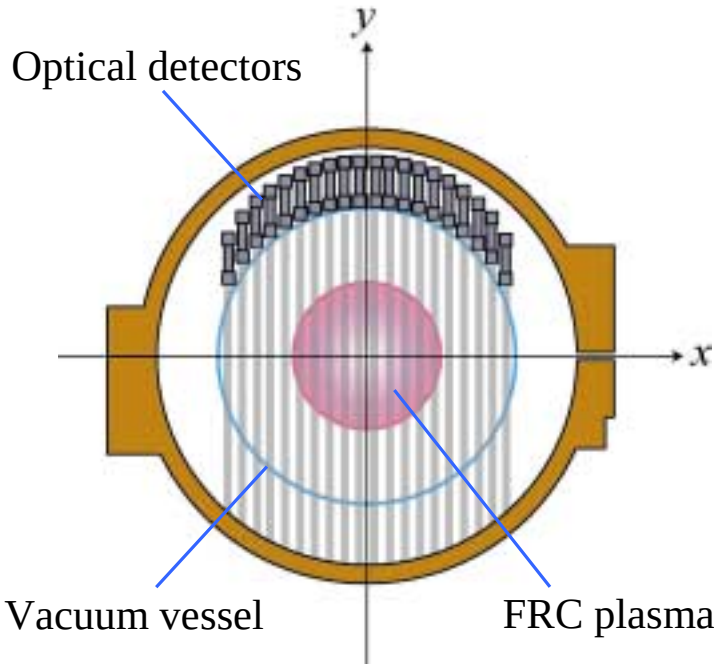

Fig. 7. Arrangement of the optical detectors at z=0.

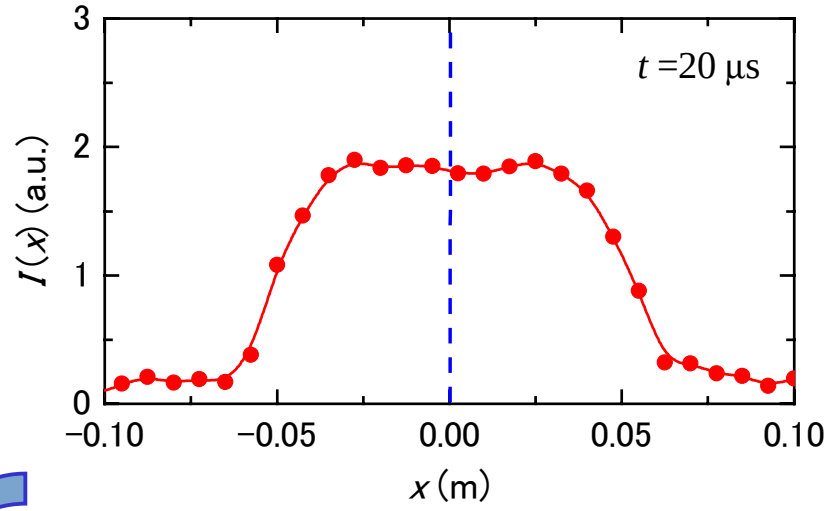

Fig. 8. Line-integrated radiation profile.

Abel inversion

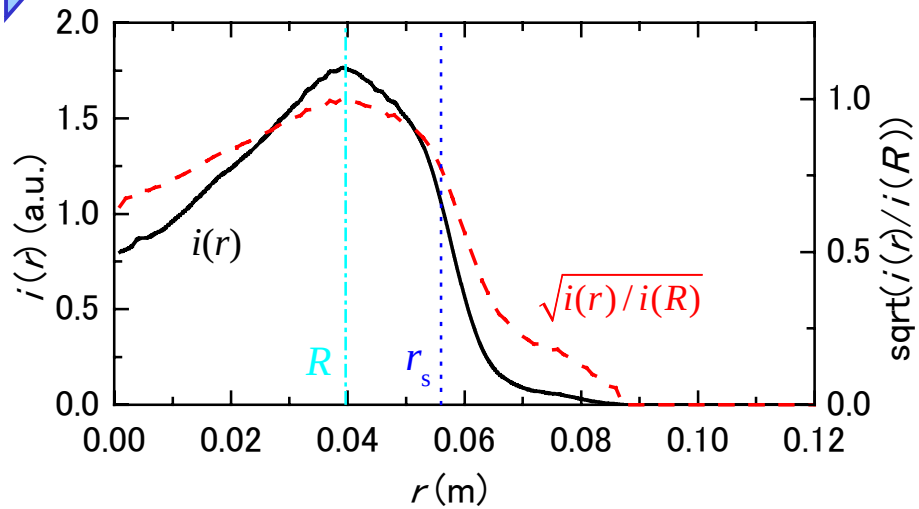

Fig. 9. Radiation power density.

***i*(*r*)** is approximately proportional to n_e^2.
β_s**=0.75** is obtained on the assumption of uniform temperature.

It is satisfied with the rigid rotor profile model at the midplane.

Abel Inversion at several axial positions

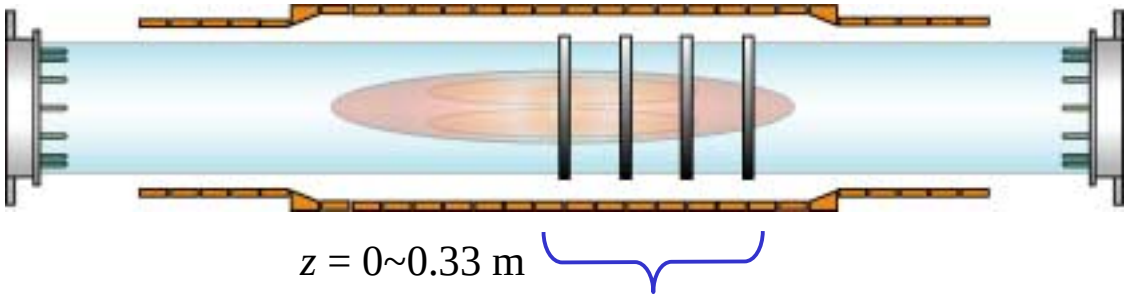

It seems that the **magnetic islands** and the **high density region** exist at **different positions** inside the separatrix.

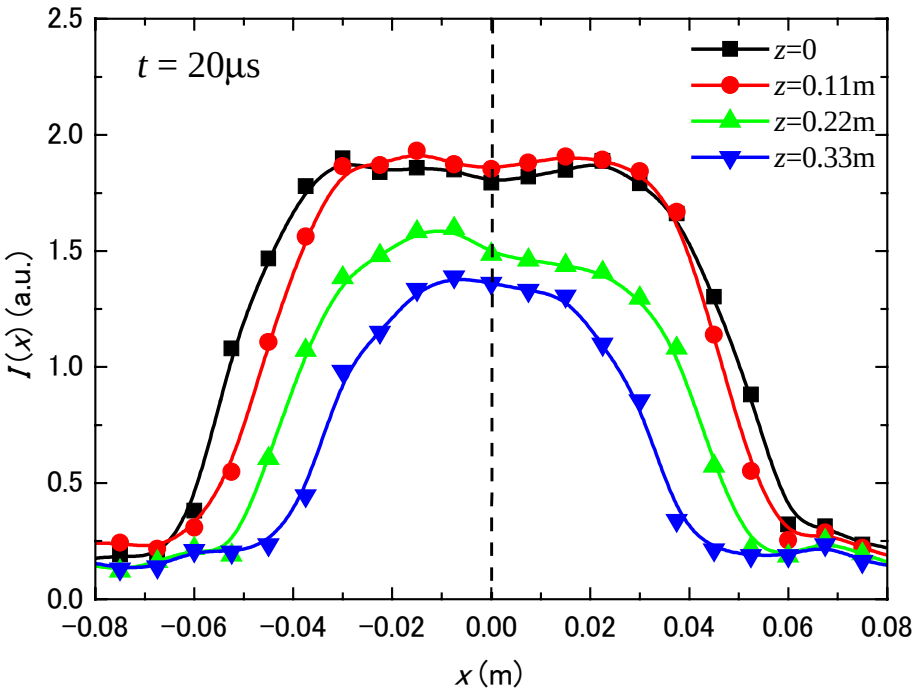

Fig. 10. Radiation profiles at four axial positions.

Abel inversion

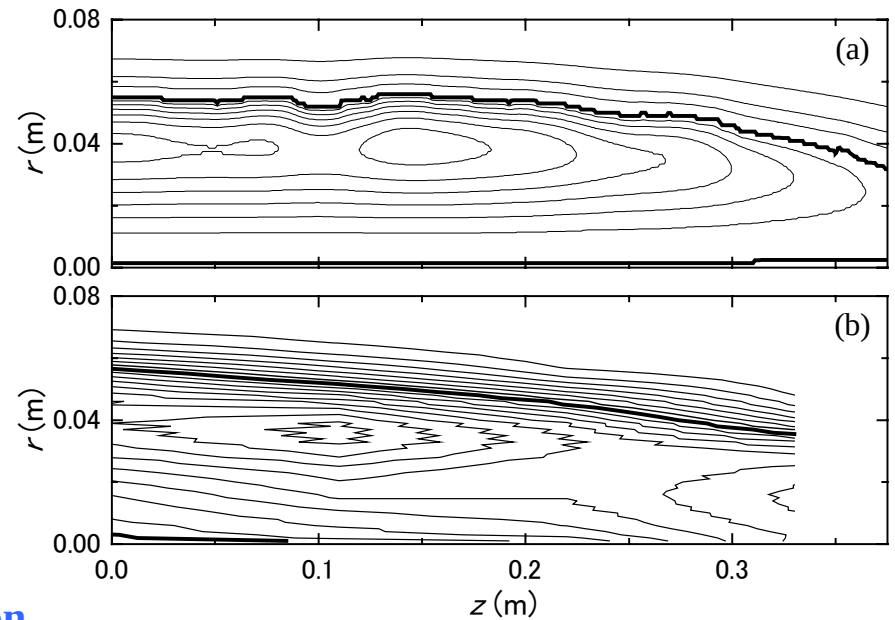

Fig. 11. (a) Flux contour of the magnetic structure and (b) contour of the normalized radiation power density.

Nonconcentric Structure

Rigid rotor profile model

$$n(x, y) = n_m \mathrm{sech}^2 \left\{ K \left[\frac{(x-\delta x)^2 + (y-\delta y)^2}{R^2} - 1 \right] \right\}$$

Where,

$$n_m = n(R),\ K = \tanh^{-1}[B(r_s)/B_0]$$

$$\delta x = \frac{\Delta_x}{r_s}(r_s - r),\ \delta y = \frac{\Delta_y}{r_s}(r_s - r)$$

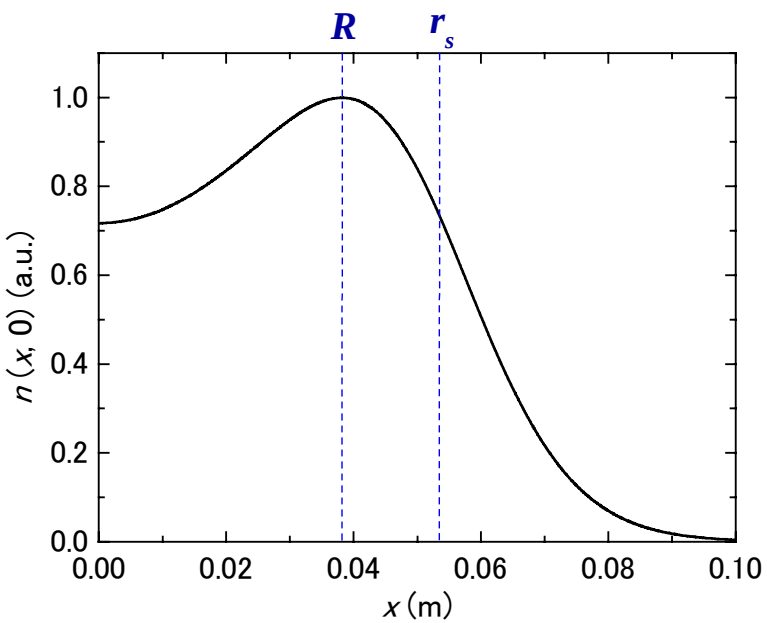

Fig. 12. Density profile. ($\delta x = \delta y = 0$)

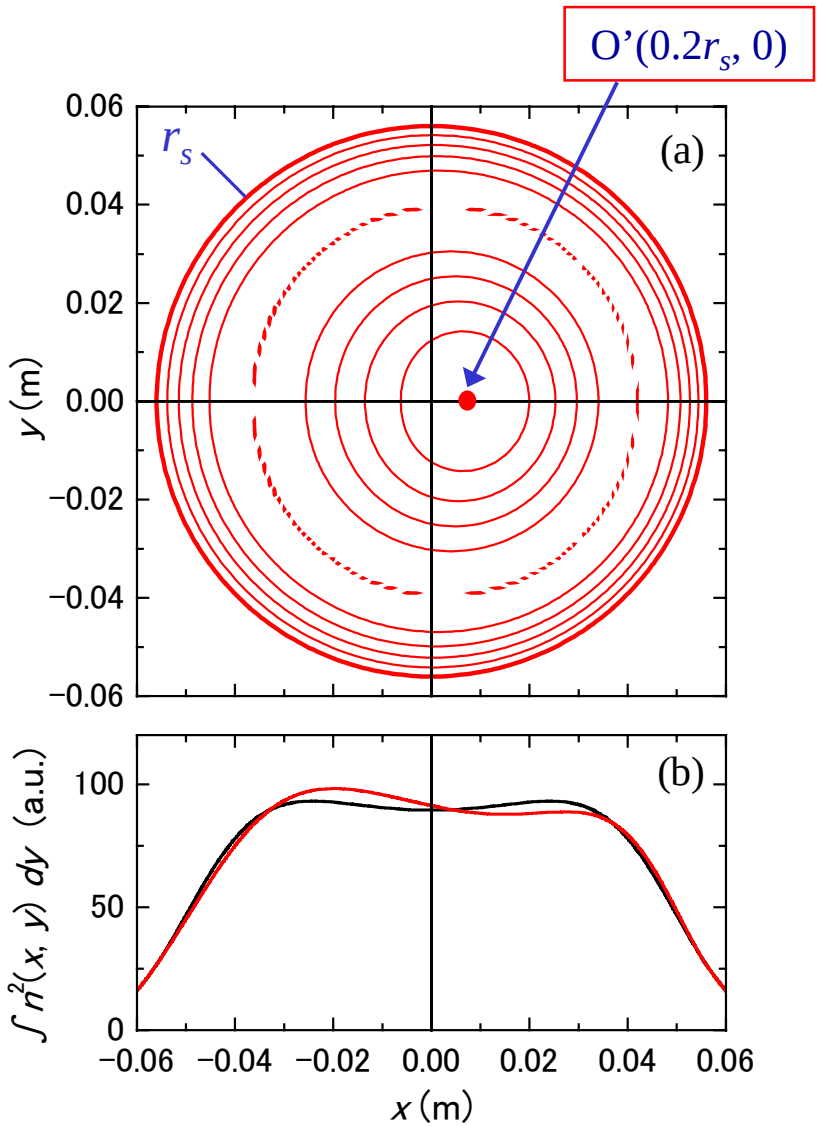

Fig. 13. (a) Contour map of the density n and (b) line-integrated n^2 profiles.

Asymmetrical Profiles

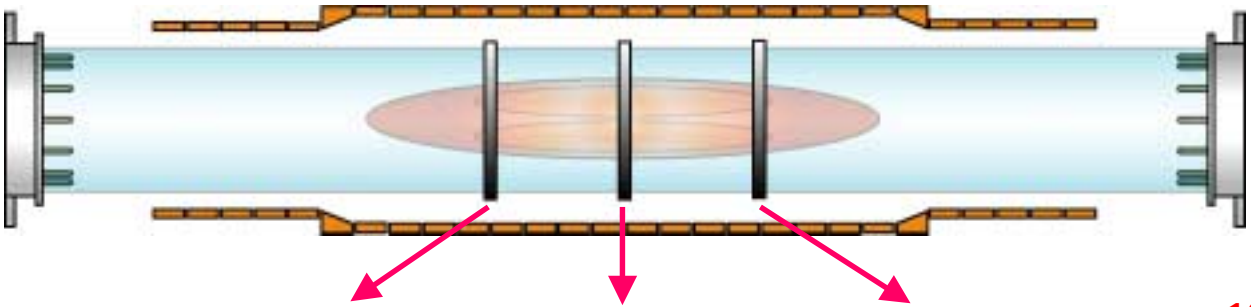

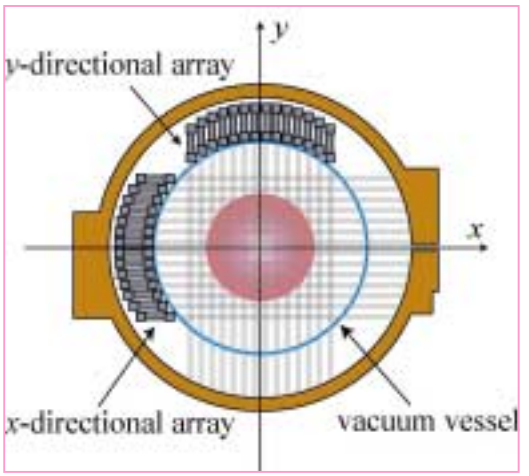

Fig. 14. Arrangement of the optical detectors.

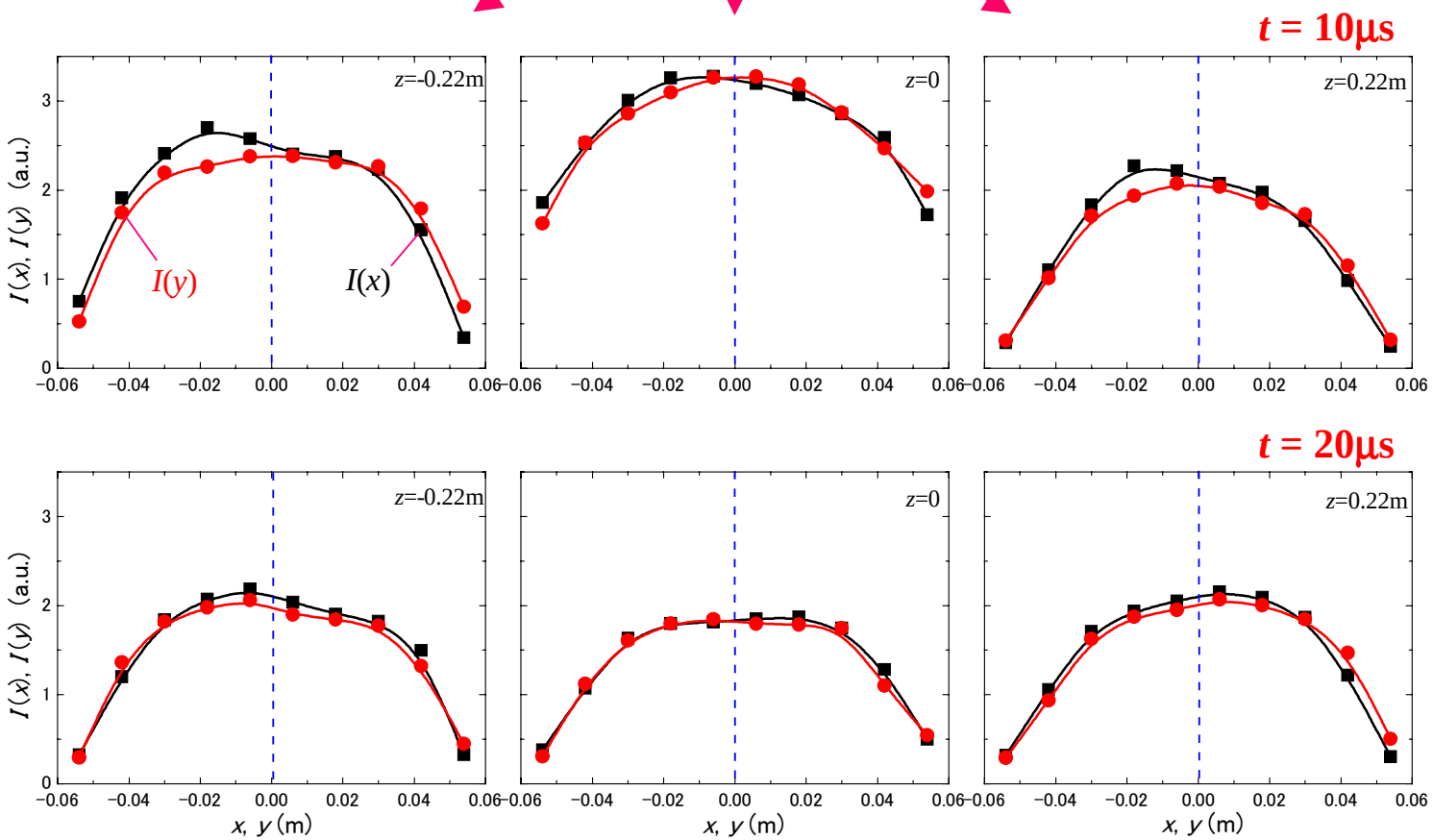

Fig. 15. Radiation intensities at three axial positions. (t=10, 20μs)

Asymmetrical Structure inside the Separatrix

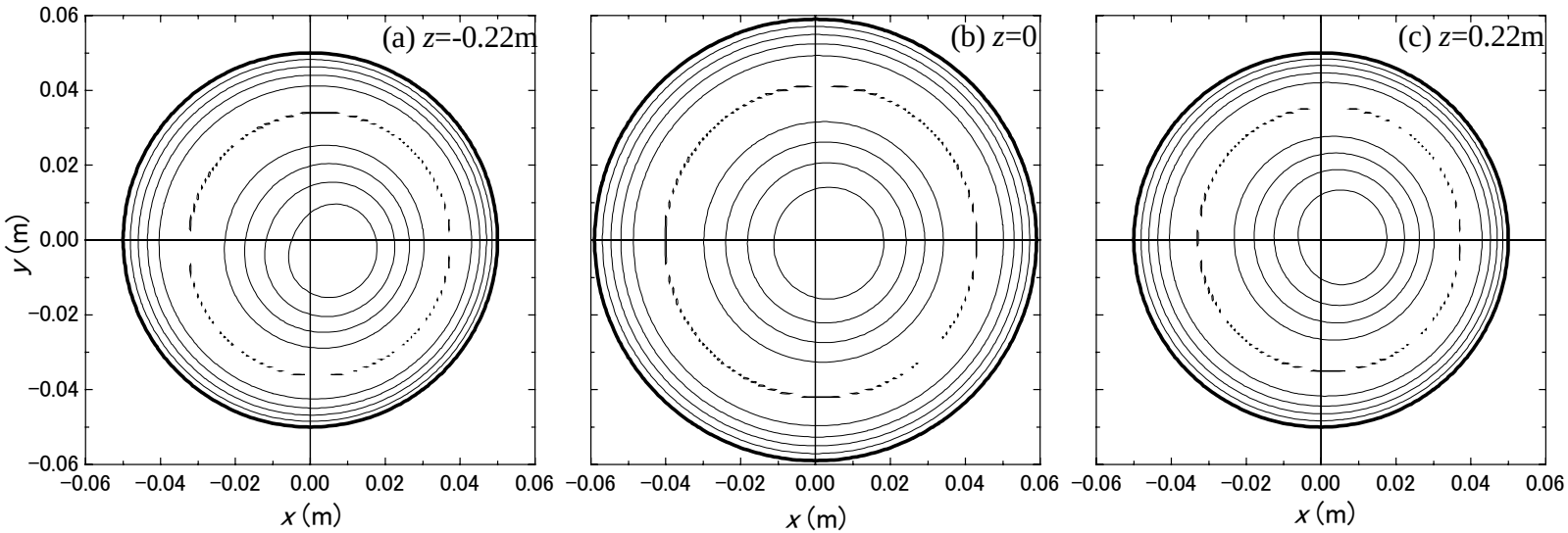

t = 10μs

Fig. 16. Nonconcentric structures at each position.

(a) r_s=0.05m, O'(0.16r_s, -0.08r_s)
(b) r_s=0.059m, O'(0.08r_s, -0.02r_s)
(c) r_s=0.05m, O'(0.15r_s, 0.02r_s)

Shift-like motion
inside the separatrix.

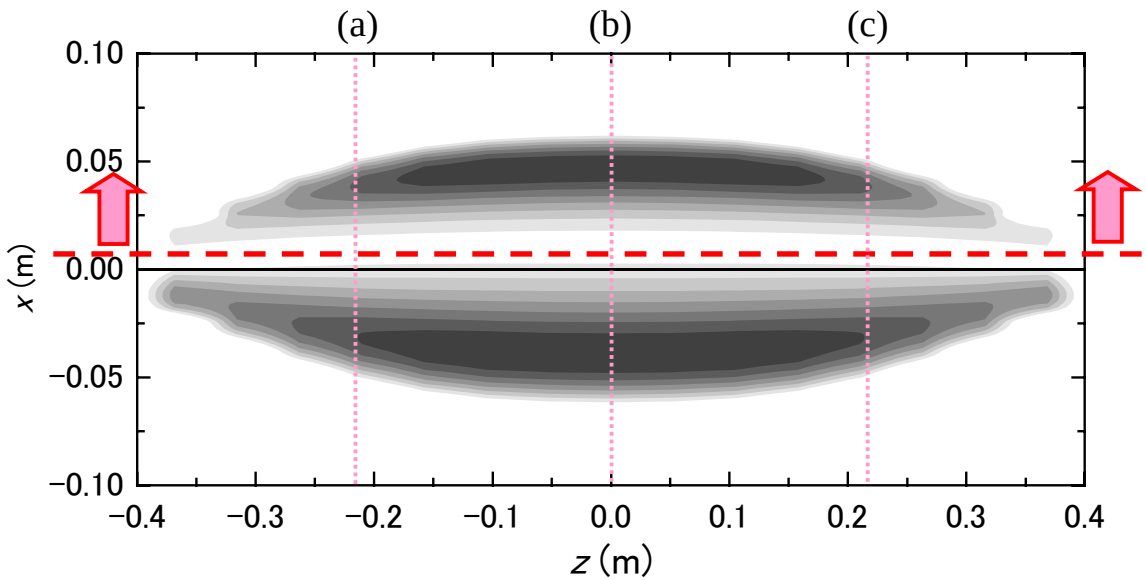

Fig. 17. Density contour map at *x*-*z* plane.

Asymmetrical Structure inside the Separatrix

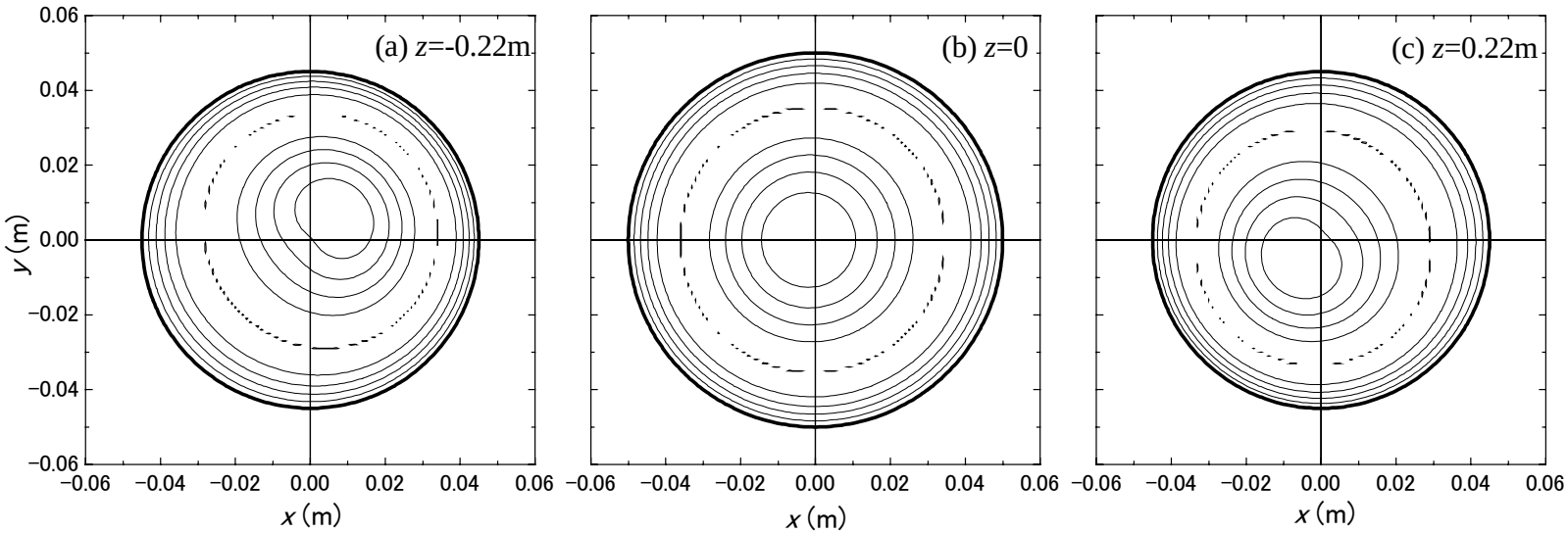

t = 20μs

Fig. 18. Nonconcentric structures at each position.

(a) r_s=0.045m, O'($0.2r_s$, $0.18r_s$)
(b) r_s=0.05m, O'($-0.05r_s$, 0)
(c) r_s=0.045m, O'($-0.16r_s$, $-0.15r_s$)

Tilt-like motion
inside the separatrix.

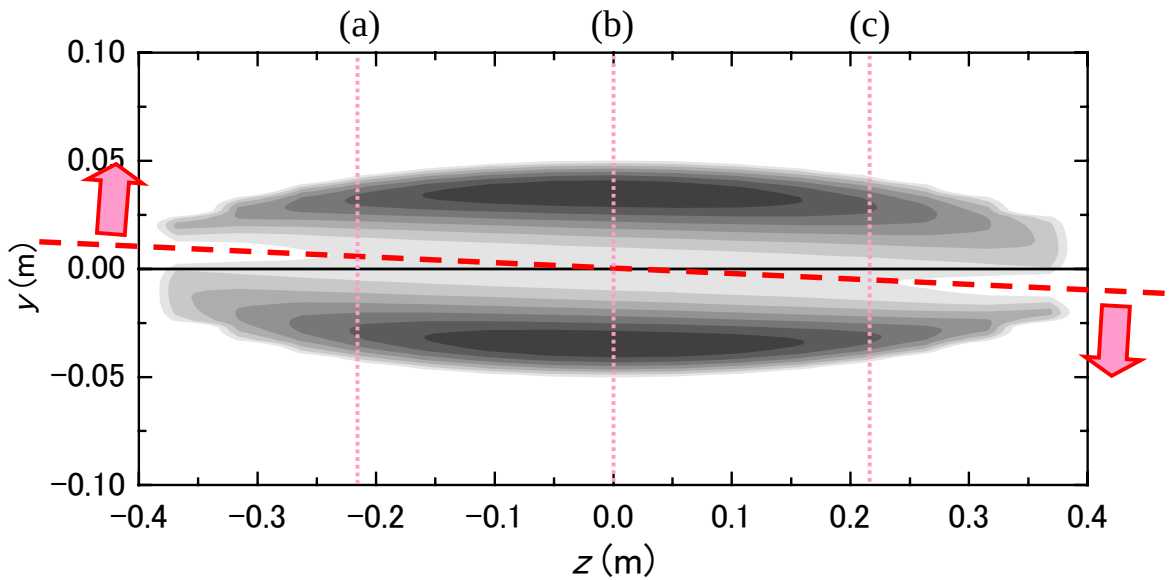

Fig. 19. Density contour map at *y*-*z* plane.

Summary

- The separatrix shape and the internal structure of FRC plasma are determined with high accuracy by comparing the measured magnetic fluxes with the Grad-Shafranov equation.
  - From the estimation of the edge-layer plasma, it is obtained that the **beta value at the separatrix** is **0.7** and the **thickness of edge-layer plasma** is **4 times the ion gyroradius**.
  - **Magnetic islands** inside the separatrix are observed at the formation phase. They **coalesce** into a large island by axial contraction, and after that, small islands **appear again** at the quiescent phase.
- In order to investigate the internal structures of FRC plasma, the radiation intensities are observed by using multichannel optical diagnostic system.
  - The radiation profiles of FRC plasma are analyzed by the **Abel inversion method**. From the analysis, the **beta value at the separatrix** is **0.75**; it relatively agrees with that of the magnetic measurement. It is satisfied with the **rigid rotor profile model** at the midplane.

Summary

- The radiation profiles of FRC plasma are observed at several toroidal cross sections.
  - As a result of the Abel inversion analysis at each axial position, it is seemed that the **high-density region** of emissivity profile and the **flux contour map** from the magnetic measurement are **different**.
  - The **asymmetrical profiles** of radiation intensity are observed at the end regions of FRC plasma. These profiles are discussed by using the modified rigid rotor profile model to estimate the effect of the internal structure. The asymmetry can be explained when the **center of nonconcentric FRC are shifted** slightly. The amount of the deviation is about 10–20% of the separatrix radius.
  - The motion inside the separatrix causes the asymmetrical profile, which is observed through the discharge. The shift-like motion and the tilt-like motion inside the separatrix are observed in the same discharge, however these **motions do not grow** as a disruptive influence on the equilibrium of FRC plasma.

Time Sequence of Asymmetrical Profiles

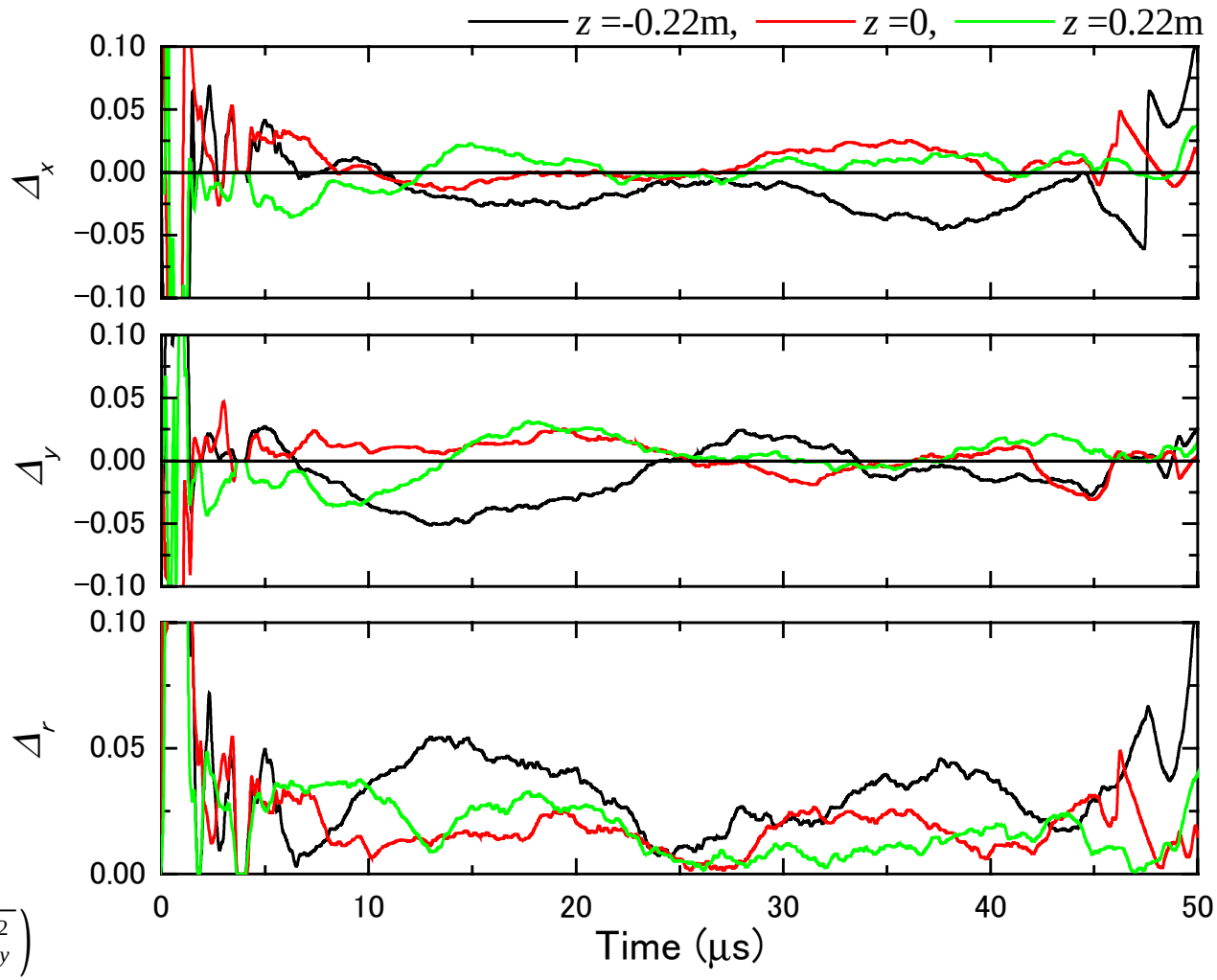

$\left(\Delta_r = \sqrt{\Delta_x^2 + \Delta_y^2}\right)$

Fig. 20. Time sequence of asymmetries at each position.

n=1 mode motion

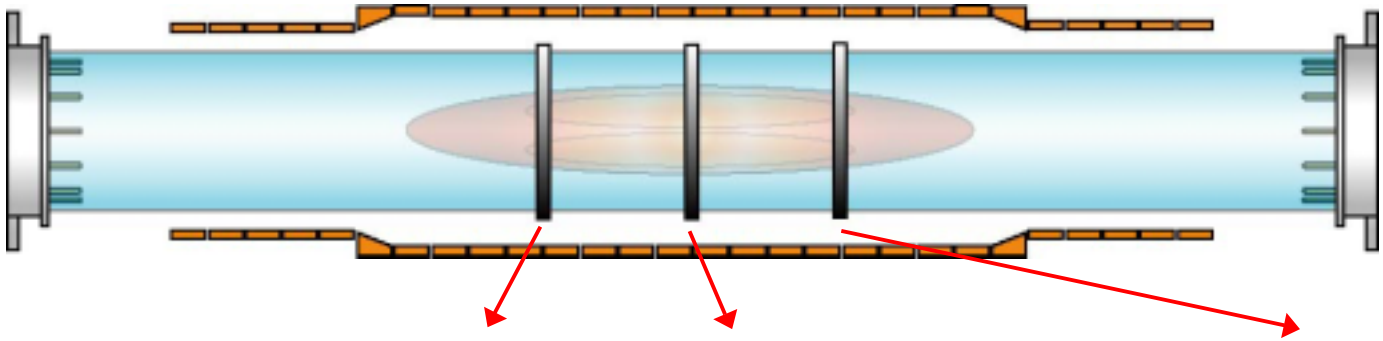

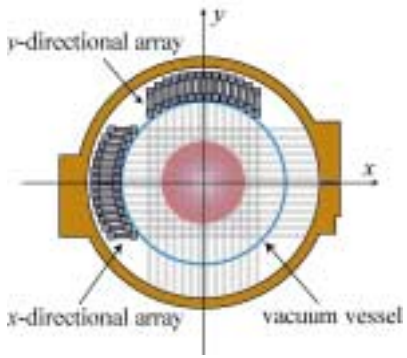

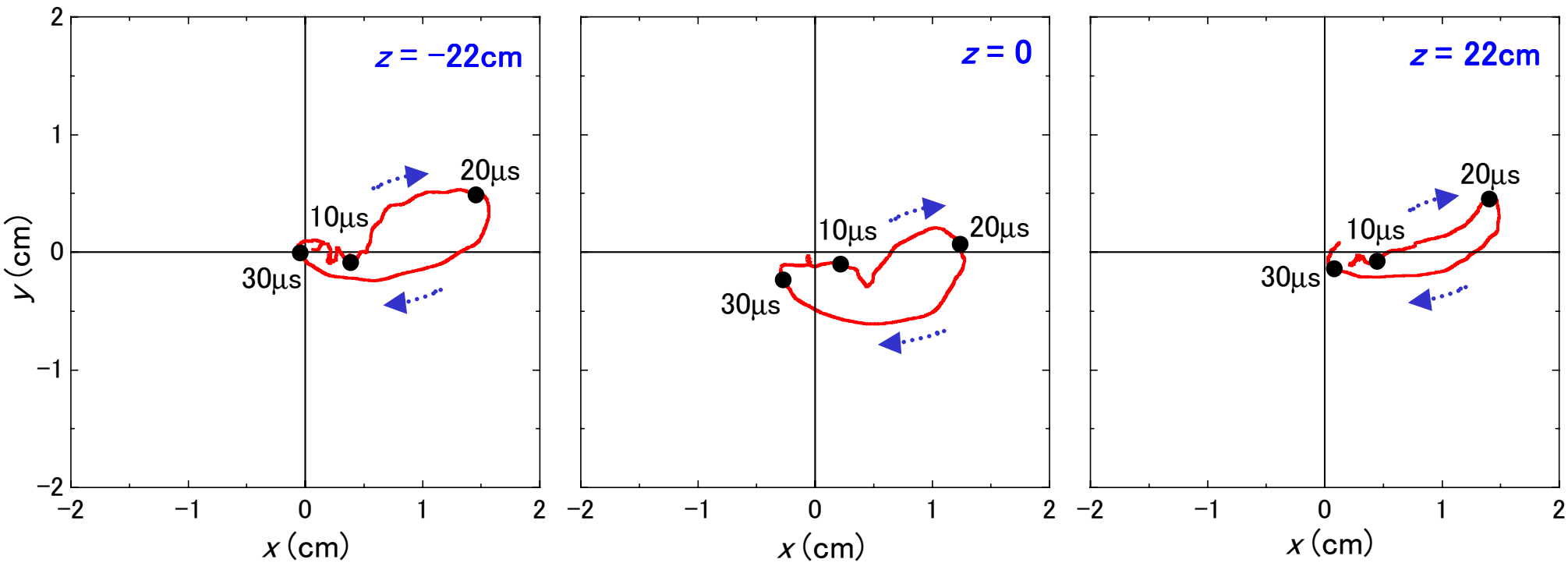

Fig. 21. Trajectories of the *n*=1 mode motion.